J. Electrochem. Sci. Eng. **10(2)** (2020) 185-198; http://dx.doi.org/10.5599/jese.732

Open Access: ISSN 1847-9286
www.jESE-online.org

Original scientific paper

Poly(vinyl alcohol)/chitosan hydrogels with electrochemically synthesized silver nanoparticles for wound dressing applications

Katarina Nešović[1], Ana Janković[1], Tamara Radetić[1], Aleksandra Perić-Grujić[1], Maja Vukašinović-Sekulić[1], Vesna Kojić[2], Kyong Yop Rhee[3], Vesna Mišković-Stanković[1,3]✉

[1]*University of Belgrade, Faculty of Technology and Metallurgy, Belgrade, Serbia*
[2]*University of Novi Sad, Faculty of Medicine, Oncology Institute of Vojvodina, Sremska Kamenica, Serbia*
[3]*Kyung Hee University, Department of Mechanical Engineering, Yongin, South Korea*

Corresponding author: ✉vesna@tmf.bg.ac.rs; Tel: + 381 11 3303 687; Fax: + 381 11 3370 387

Received: September 28, 2019; Revised: October 25, 2019; Accepted: October 28, 2019

Abstract

Polymer-based hydrogel materials are excellent candidates for new-generation wound dressings with improved properties, such as high sorption ability, good mechanical properties and low adhesiveness. Cross-linked hydrogel matrices also serve as excellent carriers for controlled release of antibacterial agents, such as silver nanoparticles (AgNPs), which are preferred over conventional antibiotics due to low propensity to induce bacterial resistance. In this work, we aim to produce novel silver/poly(vinyl alcohol)/chitosan (Ag/PVA/CHI) hydrogels for wound dressing applications. The electrochemical AgNPs synthesis provided facile and green method for the reduction of Ag^+ ions inside the hydrogel matrices, without the need to use toxic chemical reducing agents. The formation of AgNPs was confirmed using UV-visible spectroscopy, scanning and transmission electron microscopy. Release kinetics was investigated in modified phosphate buffer solution at 37 °C to mimic physiological conditions. Release profiles indicated "burst release" behavior, which is beneficial for wound dressing applications. The antibacterial activity was evaluated against Staphylococcus aureus and Escherichia coli strains using disc-diffusion test, and non-toxicity of hydrogels was proved by dye-exclusion test. The obtained results confirmed strong potential of Ag/PVA/CHI hydrogels for biomedical applications.

Keywords

Electrochemical synthesis; hydrogels; release kinetics; antibacterial activity; wound dressings

Introduction

Wound dressing materials are a major focus of biomedical and materials science research. The interest in improved material formulations is enhanced by growing problems related to treating deep and necrotic wounds and ulcers which are subject to major in-hospital infections, often caused by antibiotic and multidrug-resistant strains, sometimes with fatal consequences. Many drawbacks of traditional dressing materials (mostly textile-based) [1], such as susceptibility to bacterial infection, poor regulation of moisture, sticking to the wound tissue and frequent need for replacement, have led to a reorientation of research efforts towards new-generation polymer-based materials which should alleviate some or all of these shortcomings. Hydrophilic polymer gels are an excellent substitute for cotton-based dressings, as they provide a wealth of options to tailor such properties as adhesiveness, swelling and sorption, gas permeability, and moisture regulation [2]. Biocompatibility is always the primary characteristic that must be evaluated before these materials could be considered for such applications. Thus, several polymers (both natural-origin and synthetic) have emerged as acceptable candidates that satisfy this most important property. Among those are biocompatible and often biodegradable polymers such as alginate, chitosan (CHI), poly(vinyl alcohol) (PVA), poly(vinyl pyrrolidone) (PVP), cellulose, *etc.* [3–11]. Of course, apart from biocompatibility, hydrogel-based wound dressings must satisfy several other stringent requirements, *e.g.* sterility, non-toxicity/non-inflammatory characteristics, permeability, low adhesiveness, high sorption, moisture and temperature regulation, mechanical integrity [12]. Particularly important aspect is the method of obtaining hydrogels, as the most widely-used chemical gelation/cross-linking techniques have proved dangerous due to the use of toxic chemical gelation agents, such as glutaraldehyde, therefore, there has been substantial research on finding other, green and non-toxic cross-linkers [13]. However, an even better option would be applying physical gelation methods (which fully eliminate the need for chemical agents), such as the freezing-thawing technique, whenever applicable. Freezing-thawing is a green and simple method for obtaining hydrogels with high gelation degrees and has been widely applied for preparing poly(vinyl alcohol)-based hydrogels [14-16], although it was proved ineffective for other polymer types, such as PVP [14].

Another important aspect of wound healing problems is related to widespread antibiotics use, which has led to an alarmingly high rate of emergence of resistant bacterial strains [17]. This problem has been aggravated by systemic non-specific drug administration that requires long treatment and high doses. Hence, the research focus was shifted towards developing topical drug carriers, incorporating the antibacterial agents directly into dressing materials, thus enabling dosage decrease and allowing the drug to reach the infection site much quicker. Additionally, research is increasingly shifting away from applications of antibiotics and towards finding alternative antibacterials with less inherent risks. Thus metallic nanoparticles have emerged as strong candidates for wound-treatment applications [18]. Silver nanoparticles (AgNPs) are, by far, the most widely-used due to strong antimicrobial activity coupled with unusual and highly-tailorable properties of silver on the nano-scale [19–21]. On a note related to efforts to eliminate the toxic chemical agents for gel formation, here exists a similar concern over chemical reduction methods for obtaining AgNPs. Multiple studies were published on green reducing agents for AgNP synthesis, but one of the more promising routes is recruiting the power of electrochemistry to obtain AgNPs, either directly in the hydrogel matrix or in the colloid form [15,22–25]. The electrochemical methods of AgNP synthesis involve the reduction of silver ions using electrical current only or chemically-pure hydrogen gas which evolves due to side-reaction of water electrolysis in aqueous solutions; the final

biomaterial product is free from any side-products and thus completely non-toxic and safe for intended applications.

In this work, we present a green method for obtaining poly(vinyl alcohol) and chitosan-based hydrogel materials, which are envisioned to be used as wound dressing material, by applying physical freezing-thawing technique. Silver nanoparticles were synthesized *via* electrochemical reduction of silver ions inside the hydrogel matrix, thus obtaining a chemically-pure and non-toxic product. The successful incorporation of AgNPs was evaluated by UV-visible spectroscopy and electron microscopy; the prepared hydrogel discs were further characterized in terms of silver release behavior, as well as biological properties, *i.e.* antibacterial activity and cytotoxicity.

Experimental

For the synthesis of silver/poly(vinyl alcohol)/chitosan hydrogels, the following chemical reagents were used: fully-hydrolyzed poly(vinyl alcohol) and partially deacetylated chitosan powders (Sigma Aldrich), glacial acetic acid (Beta Hem), silver nitrate (MP Hemija), potassium nitrate (Centrohem), deionized (DI) water (Millipore).

The hydrogels were prepared following the method described in [15,25,26]. First, PVA and CHI powders were dissolved in DI water and 2.0 vol% acetic acid solutjion, respectively. The dissolution of PVA was carried out at an elevated temperature of 90 °C. After the dissolution of polymers and cooling of the PVA solution, they were mixed gradually under continuous stirring to obtain uniform PVA/CHI dispersion. The amounts of chitosan were varied, yielding two different colloid dispersions with 0.1 wt% CHI (PVA/0.1CHI) and 0.5 wt% CHI (PVA/0.5CHI). The gelation was then carried out by casting the colloid dispersions in Petri dishes and exposing them to five freezing (-18 °C for 16 h) and thawing (+4 °C for 8 h) cycles. Thus were obtained PVA/0.1CHI and PVA/0.5CHI hydrogels.

Before the AgNPs synthesis, the above-described hydrogels were swollen in $AgNO_3$ solutions supplemented with 0.1 M KNO_3 that served to improve electrical conductivity. The swelling was carried out for 48 h, after which the hydrogels were placed in an electrochemical cell depicted in Figure 1, between two parallel Pt plates that played the roles of working and counter electrodes, respectively. The electrodes were connected to a DC power source that supplied a 90 V constant voltage needed for AgNPs electrochemical synthesis. The total synthesis time was 4 min, during which the polarity of the electrodes was periodically switched (every 1 min), in order to dissolve the bulk Ag layer that was deposited on the cathode surface as a side-reaction [25]. Two different concentrations of $AgNO_3$ swelling solution were used (0.25 mM and 3.9 mM), and the obtained AgNP-incorporated hydrogels were named accordingly, *i.e.* 0.25Ag/PVA/0.1CHI and 0.25Ag/PVA/0.5CHI, or 3.9Ag/PVA/0.1CHI and 3.9Ag/PVA/0.5CHI. The hydrogels with higher amount of silver (3.9Ag/PVA/0.1CHI and 3.9Ag/PVA/0.5CHI) were used primarily for physico-chemical characterization of the hydrogels, as the higher AgNPs concentration allows better evaluation of their properties, whereas the lower-AgNP-content samples were chosen for biological evaluations, as it was confirmed in previous studies that this AgNPs concentration provided optimal balance between antibacterial properties and non-toxicity [23].

Characterization

The incorporation of AgNPs inside 3.9Ag/PVA/0.1CHI and 3.9Ag/PVA/0.5CHI hydrogels was confirmed by UV-visible spectroscopy (UV-vis); the absorbance of hydrogel discs, dissolved in DI water (1:7 w/v ratio), was measured in the wavelength range from 250 to 700 nm, using LLG-uni*SPEC* 2 (LLG Labware) instrument. Scanning electron microscopy (SEM) characterization was conducted in

field emission LEO SUPRA 55 (Carl Zeiss) microscope at 10 kV acceleration voltage. High-resolution transmission electron microscopy (HRTEM) was carried out in Talos F200X G2 (FEI) microscope at 200 kV. For HRTEM, the samples were dissolved in DI water (1:20 w/v ratio), dropped on 400-mesh copper TEM grids and left to dry for 24 h.

Silver release

The release of silver from the 0.25Ag/PVA/0.1CHI and 0.25Ag/PVA/0.5CHI hydrogel matrices was carried out according to our previously published procedure [15,26]. The hydrogel discs were immersed in 10 ml phosphate buffer (PB) solution (pH 7.4) and thermostated at 37 °C. The experiment lasted 28 days in total, during which the PB solution was removed from the vials and replaced with freshly prepared one. The removed solutions were kept in air-tight test-tubes at 4 °C before measurements. The concentrations of silver released into the PB solution were measured using PYU Unicam atomic absorption spectrophotometer (Philips). After 28 days, the hydrogels were also dissolved in 1:1 (v/v) HNO_3, and the measured concentrations represented the amount of silver that was retained inside the hydrogel after the 28-day release period.

Antibacterial properties

The antibacterial activity of PVA/0.1CHI, PVA/0.5CHI, 0.25Ag/PVA/0.1CHI and 0.25Ag/PVA/0.5CHI hydrogels was evaluated using disc-diffusion method, as described previously [15], with test strains *Staphylococcus aureus* TL and *Escherichia coli* ATCC25922. Hydrogels were sterilized under a UV-lamp for 30 min. A 0.7 wt.% soft-top agar was inoculated with overnight bacteria cultures (number of bacteria ≈10^6 CFU ml^{-1}) and poured into Petri dishes with solidified nutrient agar base. Later, the hydrogel discs were placed on the agar surface, and incubation was carried out for after 24 h at 37 °C, after which the widths of inhibition zones were measured.

Cytotoxicity

The cytotoxicity of PVA/0.1CHI, PVA/0.5CHI, 0.25Ag/PVA/0.1CHI, and 0.25Ag/PVA/0.5CHI hydrogels was evaluated using dye-exclusion test (DET), based on trypan-blue dye exclusion [27]. Two fibroblast cell lines were used – MRC-5 (human-origin) and L929 (mouse-origin). Viable cells (≈10^5 ml^{-1}) were seeded in 12-well plates, along with hydrogel disc samples. The controls were cells without the samples. The cells with hydrogels were incubated for 48 h at 37 °C, in 5 % CO_2 atmosphere. After the incubation period, the cells were separated from hydrogel samples by trypsinization, and cells were counted using a trypan blue exclusion method. The obtained cell viability results were expressed as a percent of control. All experiments were carried out in triplicate, and the results were represented as the mean ± standard deviation. Statistical significance of DET assay results was estimated using ANOVA followed by a multiple-comparison (post-hoc) test with significance level decided at $p < 0.05$.

Results and discussion

The PVA/0.1CHI and PVA/0.5CHI hydrogels were obtained by a physical cross-linking method, specifically through several cycles of freezing and thawing, during which the formation of the cross-linked polymer matrix occurred. This method is particularly advantageous for biological applications because it allows circumventing the issue of toxicity, which is always a risk in the case of chemically cross-linked hydrogels. PVA polymer has been long known for its property to form elastic and well-structured hydrogel networks through freezing-thawing technique [15,23,28–30], that can be tailored by modifying the duration, temperature, and the number of cycles to control the hydrogel

properties [28]. Another important feature of physically cross-linked hydrogels is their thermo-reversibility [31], which allows returning to sol state or dissolving them at elevated temperatures, thus significantly facilitating the handling and manipulation of the hydrogel. The gel formation is thought to occur *via* phase separation, dividing the solution into two regions, one with a high amount of polymer and a small amount of bound water, and the other *vice versa* [30–32]. Thus, cross-link sites are formed in polymer-rich phase through hydrogen bonding or micro-crystallization, resulting in a polymer network with a high gelation degree, depending of course on the polymer concentration in the starting solution, as well as on the freezing and thawing experimental conditions [29,32]. Our PVA/0.1CHI and PVA/0.5CHI hydrogels indeed had rather high gelation degrees of 94.0 % and 95.6 %, respectively, which were determined gravimetrically [25].

The synthesis of AgNPs in thus obtained physically cross-linked hydrogels was carried out by electrochemical method, well-described in our previous research [15,25–27,33]. Hydrogel disc samples were swollen in $AgNO_3$ solutions, as described in the Experimental section above. Swollen hydrogel discs were then placed in a glass cell between two platinum electrodes that were connected to a DC power supply, as depicted in Figure 1. The cathodic reactions during the synthesis can be described by equations (1) and (2), where the first reaction is the reduction of silver ions, and the second is hydrogen evolution due to the use of the aqueous solution and high applied voltage of 90 V [25]. This intense H_2 generation is what facilitates the formation of AgNPs inside the hydrogel, as the hydrogen bubbles easily permeate the hydrogel disc all across its volume, and thus the nucleation sites are formed through reaction (3) [34], with subsequent growth of nanoparticles taking place at these sites.

$$Ag^+ + e^- \rightarrow Ag \quad (1)$$

$$2H_3O^+ + 2e^- \rightarrow H_2 + 2H_2O \quad (2)$$

$$H_2 + 2Ag^+ \rightarrow 2H^+ + 2Ag \quad (3)$$

Reaction (1) mostly results in bulk silver layer deposition on the cathode surface (and perhaps the formation of a small amount of AgNPs on the hydrogel surface which is in immediate contact with the electrode). Therefore the polarity of the electrodes was switched periodically in order to dissolve this Ag layer from the cathode surface, as explained in Experimental.

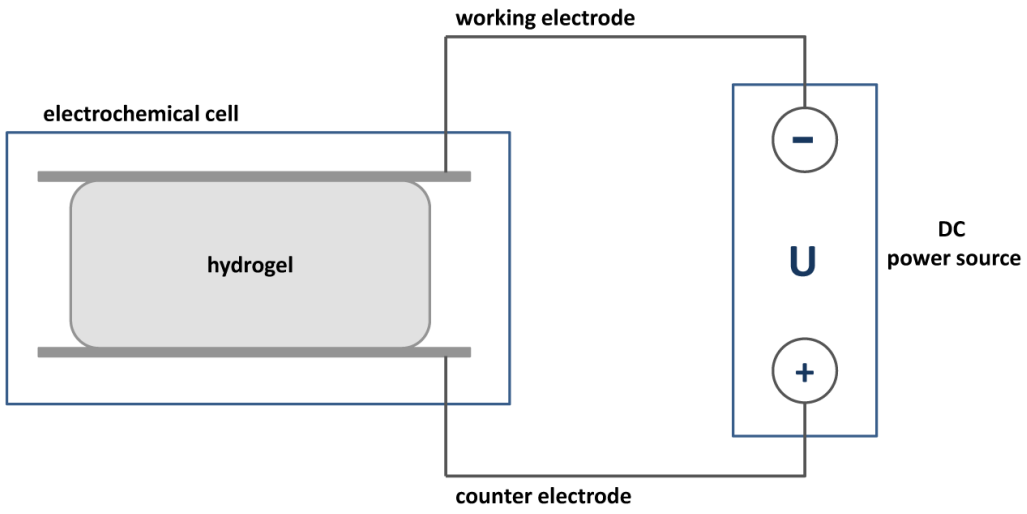

Figure 1. *Scheme of electrochemical synthesis of AgNPs in PVA/0.1CHI and PVA/0.5CHI hydrogels.*

Thus obtained 0.25Ag/PVA/0.1CHI, 0.25Ag/PVA/0.5CHI, 3.9Ag/PVA/0.1CHI and 3.9Ag/PVA/0.5CHI hydrogels were further characterized in order to confirm the formation of AgNPs, to evaluate the release of silver from their matrices and to confirm their antibacterial activity and non-toxicity.

Characterization of hydrogels

UV-visible spectroscopy was employed to confirm the presence of AgNPs inside the nanocomposite hydrogels polymer matrices. Silver nanoparticles exhibit strong absorption in the lower visible light region, which is absent from the spectra of the metal in bulk and is a consequence of the nature of nano-sized particles. The absorption is caused by matching resonance of the incident light frequency with collective oscillations of free electrons in the valence and conduction bands of silver atoms [35–37]. This phenomenon is known as localized surface plasmon resonance (LSPR), and the wavelength (λ_{max}), absorbance (A_{max}), and full-width at half maximum (FWHM) of the resulting absorption band are dependent on the type, size, shape and degree of aggregation of the nanoparticles, as well as on the properties of the surrounding medium [35,37,38]. In the case of silver nanoparticles, the LSPR band is most commonly found at wavelengths around ≈400 nm, with variations due to above-mentioned factors.

The LSPR peak in the UV-vis spectrum can, therefore, be used to evaluate the presence and the properties of AgNPs in the stabilizing matrix. Figure 2 shows the typical UV-vis spectra of 3.9Ag/PVA/0.1CHI and 3.9Ag/PVA/0.5CHI hydrogels, with prominent LSPR peaks positioned at 396 and 407 nm, respectively, which confirmed the successful synthesis of AgNPs in the hydrogels' matrices. The position and appearance of LSPR peaks agreed with the expected typical spectra of spherical AgNPs [35]. The obtained LSPR peak parameters, A_{max} and λ_{max}, were 0.21 a.u. and 396 nm for 3.9Ag/PVA/0.1CHI and 0.29 a.u. and 407 nm for 3.9Ag/PVA/0.5CHI. Further, the UV-vis spectra can be used to estimate the average diameters of AgNPs, as the properties of LSPR peaks also depend on the nanoparticles' sizes, as already mentioned above. The AgNPs diameters (d_{AgNP}) could be estimated based on FWHM of the LSPR peak [25,39]. The FWHM values were obtained by fitting the UV-vis spectra with Gaussian-type curves after background subtraction (Figure 2), and the obtained values were 68.2 nm for 3.9Ag/PVA/0.1CHI and 79.8 nm for 3.9Ag/PVA/0.5CHI. Thus, AgNP diameters for 3.9Ag/PVA/0.1CHI and 3.9Ag/PVA/0.5CHI hydrogels were estimated to be 10.1 nm for 3.9Ag/PVA/0.1CHI and 11.8 nm for 3.9Ag/PVA/0.5CHI. These results indicated that the AgNPs diameters were in the range of ≈10 nm, which is beneficial for envisioned antibacterial applications. It was also observed that the maximum absorbance was higher in the case of 3.9Ag/PVA/0.5CHI, indicating higher concentration of AgNPs incorporated inside the hydrogel with higher chitosan content.

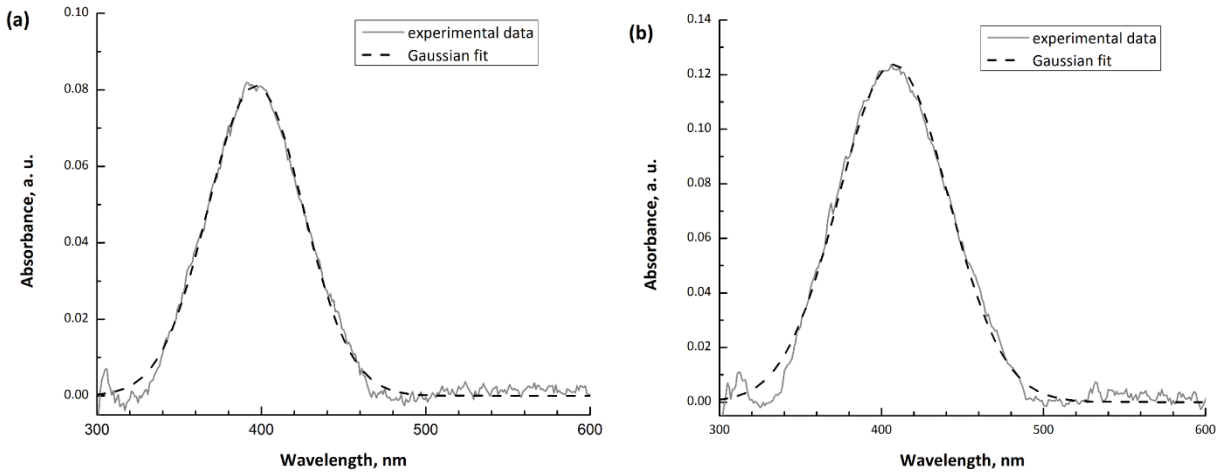

Figure 2. *UV-visible spectra of* ***(a)*** *3.9Ag/PVA/0.1CHI and* ***(b)*** *3.9Ag/PVA/0.5CHI hydrogels.*

Further confirmation of AgNPs incorporation and stabilization inside hydrogel matrices was obtained by electron microscopy. FESEM micrographs of 3.9Ag/PVA/0.1CHI and 3.9Ag/PVA/0.5CHI hydrogels, presented in Figure 3a and 3b, respectively, showed smooth hydrogel surface at high magnification, with AgNPs uniformly distributed in the polymer matrix. HRTEM images (Figure 3c and 3d) confirmed the crystalline structure of AgNPs which were mostly sized between 5 and 10 nm. However, HRTEM also indicated the presence of larger nanoparticles, as well as some aggregation (not shown). This was also confirmed by dynamic light scattering analysis (DLS) that pointed to monomodal size distribution along the hydrogel volume [25]. DLS also provided statistically averaged values of AgNPs hydrodynamic diameters of 7.33 ± 0.088 nm for (3.9Ag/PVA/0.1CHI) and 6.11±0.10 nm (3.9Ag/PVA/0.5CHI), along with polydispersity indices of 0.211 and 0.269, respectively [25].

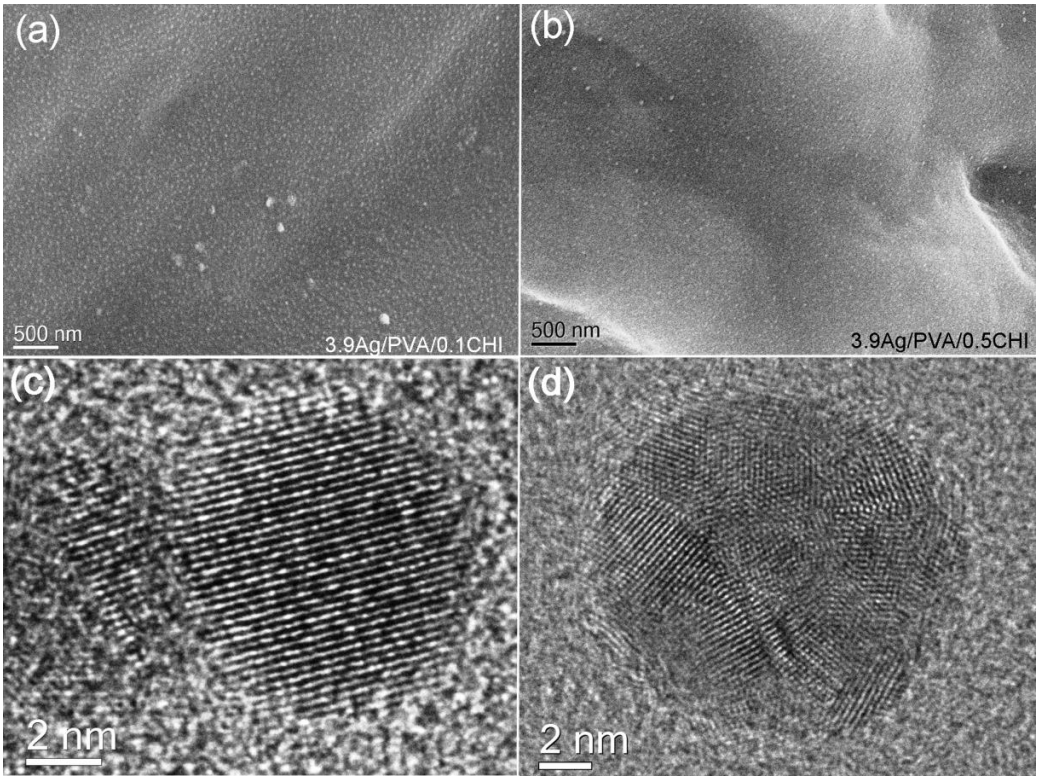

Figure 3. ***(a, b)*** *FESEM and* ***(c, d)*** *HRTEM micrographs of* ***(a, c)*** *3.9Ag/PVA/0.1CHI and* ***(b, d)*** *3.9Ag/PVA/0.5CHI hydrogels.*

Silver release

The release of the active antibacterial component from the hydrogel matrix, and the ability to control the release dynamics are important properties that are always evaluated when designing a new wound dressing material. The ability of the hydrogel to provide sufficient and sustained inflow of antibacterial agent to the wound site is also one of the factors that dictate durability of the dressing, *i.e.* determine the period after which the dressing should be replaced. Usually, the release of drug from hydrogel matrix follows a two-stage profile, with the very fast initial release, known as "burst" period, and a latter slower release period when the remnants of the drug are released from the matrix. The AgNPs release from 0.25Ag/PVA/0.1CHI and 0.25Ag/PVA/0.5CHI hydrogel matrices followed this expected trend, as shown in their release profiles in Figures 4a and 5a, respectively. The initial concentrations of silver in hydrogels were 81.5 mg dm^{-3} for 0.25Ag/PVA/0.1CHI, and 87.2 mg dm^{-3} for 0.25Ag/PVA/0.5CHI, and after this 28-day monitored period, the remaining concentrations were 21.1 and 21.0 mg dm^{-3}, respectively (Figures 4a and 5a). It can be observed that, even though the hydrogel with 0.5 wt% CHI initially contained slightly higher amount of AgNPs

(as also confirmed by UV-vis), the release profiles were similar for both hydrogels, and the remaining concentration was basically the same.

The release profiles can be fitted with different models in order to elucidate kinetic and diffusion mechanisms, *e.g.* with such widely-used models as Korsmeyer-Peppas and Makoid-Banakar [25]. Here, we will discuss several basic kinetic models, *i.e.* zero, first and second-order, in order to determine the dominant kinetic mechanism of silver release and to compare the obtained kinetic parameters. The zero-order kinetics represents a process where release rate is constant and independent of both time and concentration of the drug being released, and can be described by equation (4), where $c_{Ag,0}$ is the initial concentration of silver in the hydrogel, c_{Ag} is the concentration of silver remaining in the hydrogel after release time t and k_0 is the rate constant of zero-order release.

$$c_{Ag} = c_{Ag,0} - k_0 \cdot t \quad (4)$$

On the other hand, the rate of first-order release process depends linearly on the concentration of AgNPs being released, while c_{Ag} in the hydrogel decreases exponentially with time. Such process can be represented by equation (5), where k_1 is the rate constant of first-order release:

$$c_{Ag} = c_{Ag,0} \cdot \exp(-k_1 \cdot t) \quad (5)$$

The equation (5) can be rearranged by taking the logarithm of both sides of the equation, yielding the linear dependence of $\ln(c_{Ag})$–t:

$$\ln c_{Ag} = \ln c_{Ag,0} - k_1 \cdot t \quad (6)$$

Finally, in second-order processes, the release rate follows square-law dependence on the AgNPs concentration, whereas the concentration itself is inversely proportional to the release time. The second-order release kinetics can be described using the following equation:

$$\frac{1}{c_{Ag}} = \frac{1}{c_{Ag,0}} + k_2 t \quad (7)$$

where k_2 is the second-order rate constant. The obtained release profiles of 0.25Ag/PVA/0.1CHI and 0.25Ag/PVA/0.5CHI hydrogels and corresponding fits are presented in Figures 4 and 5.

Using zero-order and first-order kinetic models, it was impossible to fit the entire release period, however, the profiles were divided into two, previously described release periods – initial burst release and subsequent slower process. These two periods could be fitted well with both zero and first-order kinetics, as shown in Figures 4b and 4c (0.25Ag/PVA/0.1CHI), as well as 5b and 5c (0.25Ag/PVA/0.5CHI), respectively. As anticipated, the obtained rate constants in the initial period (k_0 values of 1.5×10^{-3} and 1.6×10^{-3} mg dm^{-3} s^{-1} for 0.25Ag/PVA/0.1CHI and 0.25Ag/PVA/0.5CHI, respectively, and k_1 values of 2.0×10^{-5} s^{-1} for both hydrogels) were larger than those for release in later times ($k_0 = 0.3\times10^{-3}$ mg dm^{-3} s^{-1} and $k_1 = 9.0\times10^{-6}$ s^{-1} for both hydrogels), confirming the "burst effect" during short-time release. On the other hand, the second-order model perfectly fitted the obtained release profiles during the entire monitored period for both 0.25Ag/PVA/0.1CHI and 0.25Ag/PVA/0.5CHI (Figures 4d and 5d, respectively), with R^2 values of 0.991 and 0.995, indicating that the release of silver nanoparticles from these hydrogels follows second-order kinetics. The obtained value for second-order rate constant was 3.0×10^{-7} dm^3 mg^{-1}s^{-1} for both 0.25Ag/PVA/0.1CHI and 0.25Ag/PVA/0.5CHI hydrogels, pointing to relatively slow and gradual silver release over the 28days.

The obtained silver release results confirmed a strong potential of 0.25Ag/PVA/0.1CHI and 0.25Ag/PVA/0.5CHI hydrogels for wound dressing applications. The initial "burst release" period lasted even up to 5 days (Figures 4a and 5a), enabling the prolonged use of hydrogel dressing, limiting the need for the replacement that could aggravate the newly formed tissue and cause damage to the wound.

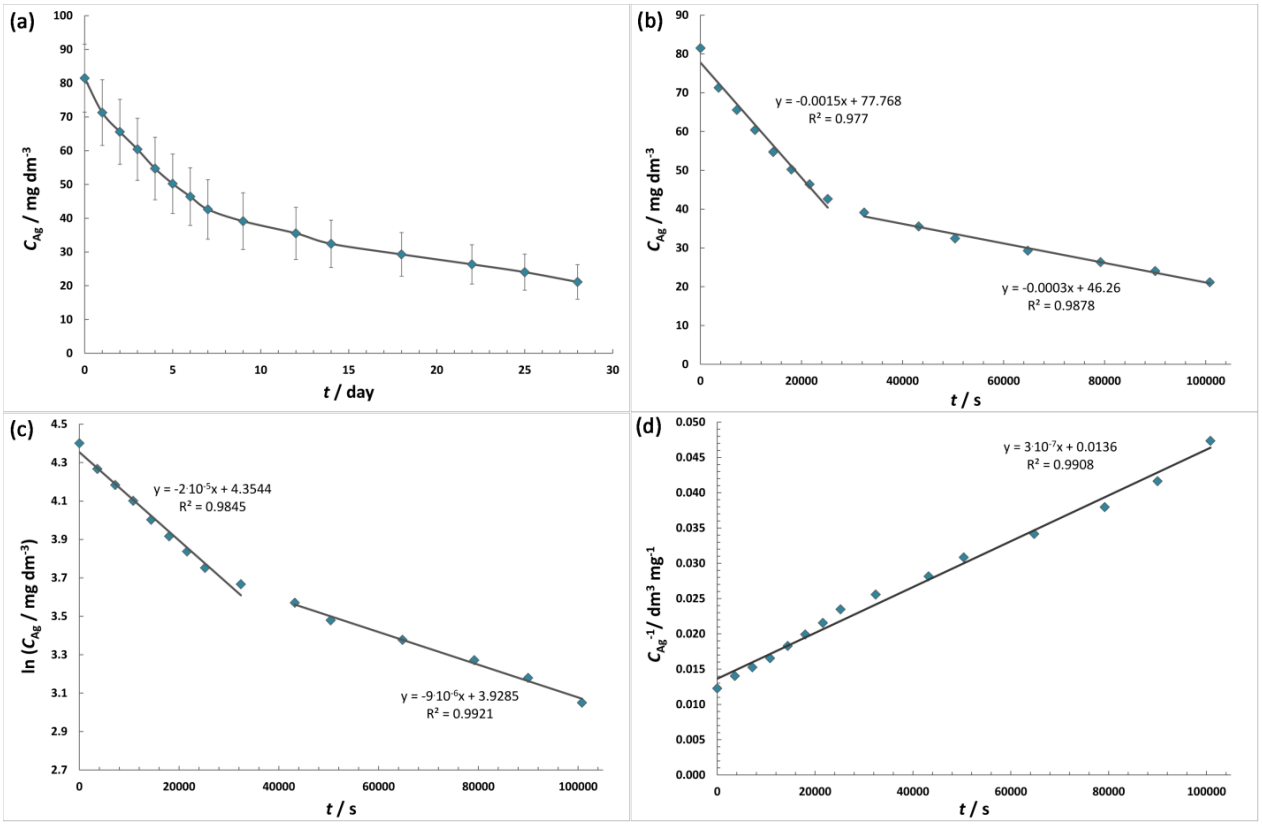

Figure 4. *Silver release of 0.25Ag/PVA/0.1CHI hydrogel:* ***(a)*** *silver release profile,* ***(b)*** *zero-order fit,* ***(c)*** *first-order fit and* ***(d)*** *second-order fit.*

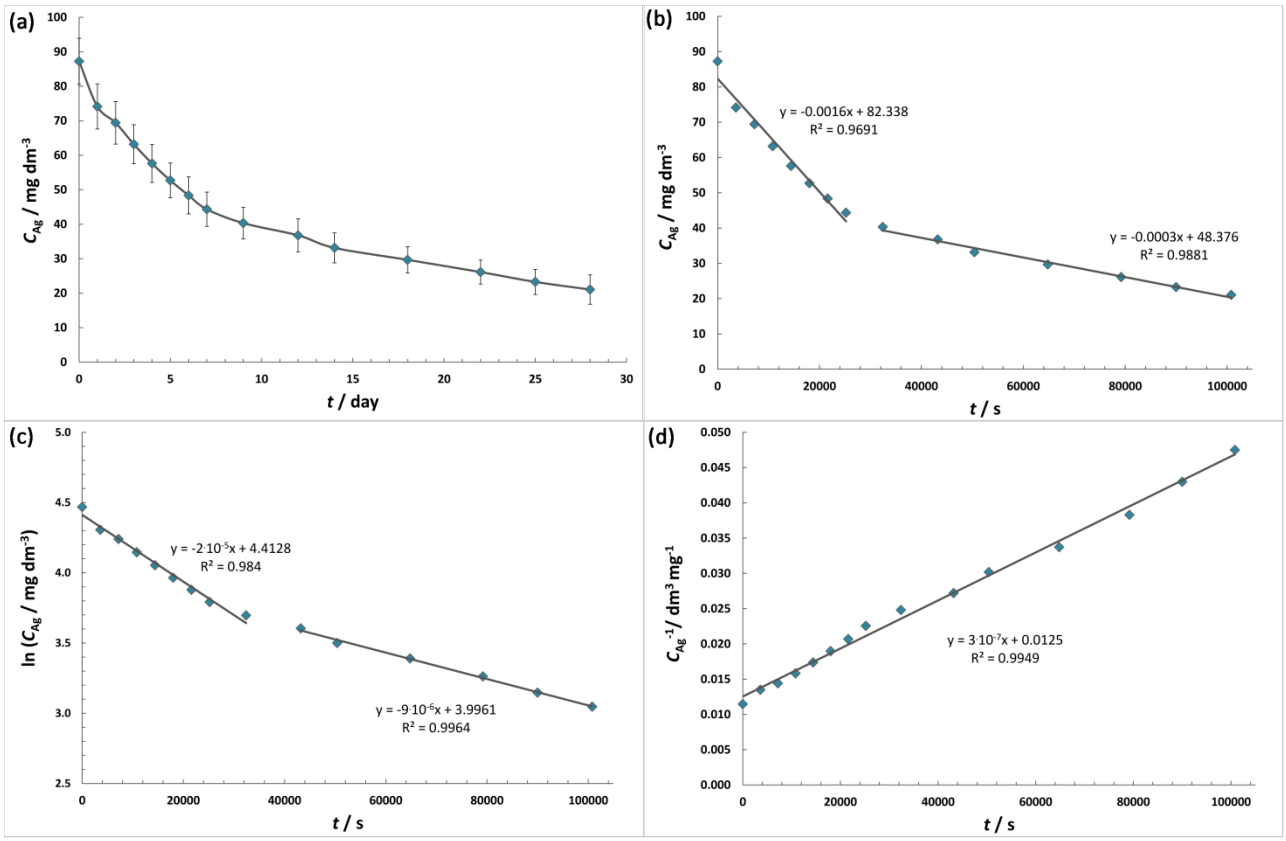

Figure 5. *Silver release of 0.25Ag/PVA/0.5CHI hydrogel:* ***(a)*** *silver release profile,* ***(b)*** *zero-order fit,* ***(c)*** *first-order fit and* ***(d)*** *second-order fit.*

The obtained silver release results confirmed a strong potential of 0.25Ag/PVA/0.1CHI and 0.25Ag/PVA/0.5CHI hydrogels for wound dressing applications. The initial "burst release" period

lasted even up to 5 days (Figures 4a and 5a), enabling the prolonged use of hydrogel dressing, limiting the need for the replacement that could aggravate the newly formed tissue and cause damage to the wound. Further, the governing mechanism of release was found to be second-order kinetics, where the time of release is inversely proportional to the concentration of AgNPs in the dressing, meaning that the release rate slows down in later periods, thus preventing potential "accumulated-effect" or repeated-dose toxicity.

Antibacterial activity

The antibacterial efficiency of PVA/0.1CHI, PVA/0.5CHI, 0.25Ag/PVA/0.1CHI and 0.25Ag/PVA/0.5CHI hydrogels was investigated using disc-diffusion test against two most common causes of wound infections – *S. aureus* and *E. coli*. The samples were incubated on top of bacteria-inoculated agar plates, and inhibition zones were measured from photographs using AutoCAD® software. The obtained widths of inhibition zones (minus the sample diameters, as the samples differed slightly in size) are summarized in Table 1. All hydrogels exhibited antibacterial activity against *S. aureus*. The antibacterial activity of hydrogels without AgNPs occurred due to the presence of chitosan, which is known as a good antibacterial agent [40]. On the other hand, the presence of AgNPs improved hydrogels' antibacterial efficiency, and the widths of inhibition zones increased to 0.9 mm for 0.25AgPVA/0.1CHI and 1.3 mm for 0.25AgPVA/0.5CHI (Table 1). The 0.25AgPVA/0.5CHI exhibited slightly more pronounced antibacterial action, evidencing the synergistic effect of chitosan and silver nanoparticles. However, in the case of *E. coli*, the antibacterial effect was not as pronounced. PVA/0.1CHI hydrogel did not exhibit any antibacterial activity, supposedly because the amount of CHI was not enough to cause growth inhibition of *E. coli* strain, which is generally more resistant than our *S. aureus* strain. The inhibition zone of PVA/0.5CHI hydrogel was 0.7 mm wide, due to the higher amount of chitosan in the hydrogel. The widest inhibition zone was around 0.25Ag/PVA/0.1CHI (1.2 mm) indicating that the incorporation of AgNPs improved antibacterial activity of the hydrogel, whereas it decreased for 0.25Ag/PVA/0.5CHI (0.5 mm). The discrepancies in the width of inhibition zones are linked to the hydrogel samples swelling during the 24 h experimental period that comes as an artifact of soft-top agar moisture content. Hydrogel samples swelling shielded the propagation and it was difficult to differentiate between the zones of bacterial sensitivity.

Table 1. *Widths of inhibition zones around the samples for PVA/0.1CHI, PVA/0.5CHI, 0.25Ag/PVA/0.1CHI and 0.25Ag/PVA/0.5CHI hydrogels and for both tested bacterial strains (S. aureus and E. coli).*

Sample	Inhibition zone width, mm	
	S. aureus	*E. coli*
PVA/0.1CHI	0.6	/
PVA/0.5CHI	0.7	0.7
0.25AgPVA/0.1CHI	0.9	1.2
0.25AgPVA/0.5CHI	1.3	0.5

Overall, the obtained hydrogels exhibited antibacterial activity, which was also confirmed by the test in suspension from our previous work [25], where it was shown that 0.25Ag/PVA/0.1CHI and 0.25Ag/PVA/0.5CHI hydrogels caused complete reduction of *E. coli* and *S. aureus* colonies after 1 h. These results indicated that the new wound dressing materials presented here could be considered as good candidates for antibacterial applications.

Superior antibacterial action of AgNPs compared to the bulk metal stem from advanced physiochemical and biological properties. The exact mechanism of action, although not conclusively

known, is thought to lean on two intertwined phenomena, first being the effect of direct contact between AgNPs and bacterial cell, while the second comes as the result of ion release-mediated antibacterial activity [41]. AgNPs can penetrate the bacterial membrane, causing physical damage, subsequent cellular contents leakage and bacterial death [42,43]. Another significant contribution to enhanced AgNPs antibacterial activity is their size, as smaller nanoparticles provide for larger contact area for interaction with the bacterial cells [41]. Inside the bacterial cell, AgNPs interact with cellular structures and proteins, lipids, enzymes, ribosomes and DNA, inevitably leading to bacterial dysfunction and finally apoptosis [43–45]. AgNPs could also cause increased production of high amounts of reactive oxygen and free radical species and reduce the ability of bacteria to produce antioxidant enzymes [45]. The high-surface area AgNPs can also sustainably release of Ag^+ ions, which could affect ATP production and inhibit normal cellular processes through binding to some membrane proteins or by chelating with nucleic acids [45]. Thus, AgNPs possess exceptionally strong antibacterial activity achieved through the dual mechanism of direct interactions with bacterial cells, as well as the release of reactive silver ions.

Cytotoxicity

The cytotoxicity of PVA/0.1CHI, PVA/0.5CHI, 0.25Ag/PVA/0.1CHI and 0.25Ag/PVA/0.5CHI hydrogels was evaluated using dye-exclusion test, which is based on a principle that only non-viable or dead cells take up the trypan-blue dye, whereas the viable cells (with membrane integrity intact) do not [46]. The cell viability was expressed as a percentage of control, and the results are presented in Figure 6.

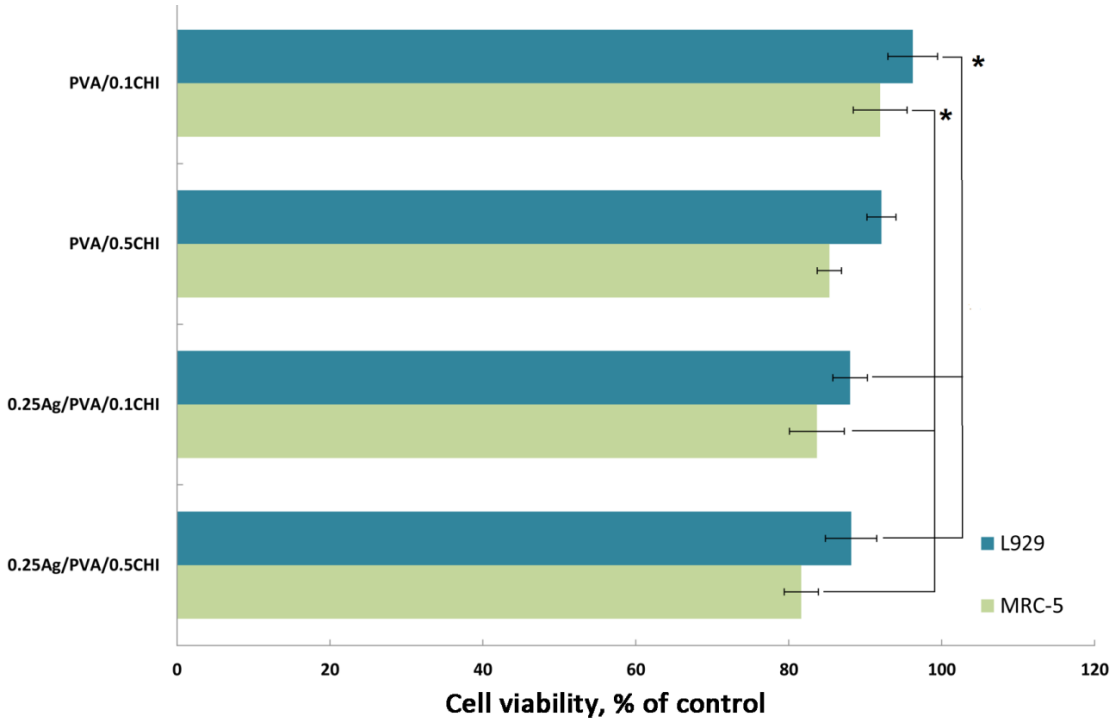

Figure 6. *DET test of cytotoxicity towards MRC-5 and L929 cell lines for PVA/0.1CHI, PVA/0.5CHI, 0.25Ag/PVA/0.1CHI and 0.25Ag/PVA/0.5CHI hydrogels. *significant differences ($p < 0.05$) were observed between the indicated samples, within the respective cell line.*

From the obtained data, it can be observed that both cell lines exhibited high survival rates in the presence of all investigated samples, confirming their non-toxicity towards both mice and human cells. The viabilities of L929 cell line were 96.21, 92.12, 88.0 and 88.15 %, and MRC-5 exhibited viabilities of 91.95, 85.31, 83.67 and 81.63 %, for PVA/0.1CHI, PVA/0.5CHI, 0.25Ag/PVA/0.1CHI and

0.25Ag/PVA/0.5CHI, respectively. According to the statistical analysis, 0.25Ag/PVA/0.1CHI and 0.25Ag/PVA/0.5CHI hydrogels exhibited significant decrease in viability ($p < 0.05$), compared to PVA/0.1CHI (Figure 6), however, the cell survival rates were still higher than 80 % (almost 90 % for L929), so all hydrogels could be classified as non-cytotoxic or mildly cytotoxic, according to a cytotoxicity scale [47]. Similar results were obtained using MTT assay [25], confirming strong biocompatibility of the synthesized hydrogels, and, coupled with their potent antibacterial activity, excellent potential for wound dressing applications.

Conclusions

In this work, we have synthesized poly(vinyl alcohol) and chitosan polymer blend hydrogels aimed for wound dressing materials. The amount of chitosan in the hydrogel was varied (0.1 wt% and 0.5 wt%) in order to evaluate its effect on the properties of the obtained materials. Thus, PVA/0.1CHI and PVA/0.5CHI hydrogels were obtained by green freezing-thawing method during 5 consecutive cycles, which yielded high gelation degrees of 94.0 % and 95.6 %, respectively.

Incorporation of silver nanoparticles was achieved *in situ*, inside the matrices of the obtained hydrogels, previously swollen in Ag^+ aqueous solution. The Ag^+ ions were reduced to AgNPs using the electrochemical method at a constant voltage of 90 V. The successful impregnation of AgNPs was confirmed by UV-visible spectroscopy and scanning electron microscopy, whereas transmission electron microscopy indicated the formation of AgNPs with diameters around ≈10 nm. The release of silver from 0.25Ag/PVA/0.1CHI and 0.25Ag/PVA/0.5CHI hydrogels was investigated over 28 days and pointed to two-stage release behavior, with initial "burst release" followed by a slower period after the amount of silver decreased in the hydrogel. The mechanistic study, carried out by fitting with different kinetic models, yielded the conclusion that the overall release followed second-order mechanism, with the calculated rate constant of 3.0×10^{-7} dm^3 mg^{-1} s^{-1}. Antibacterial properties were proven against *S. aureus* and *E. coli* using the disc-diffusion method, whereas the DET assay confirmed the absence of cytotoxic effects towards MRC-5 and L929 fibroblast cell lines.

In summary, based on the presented results, the obtained hydrogels were proven to be strong candidates for wound dressing materials applications, in the light of their highly favorable properties of silver release, antibacterial activity, and non-toxicity.

***Acknowledgements**: The authors thank Ministry of Education, Science, and Technological Development Serbia, (grant No. III45019) and the National Research Foundation of the Ministry of Education, Republic of Korea (Basic Science Research Program grant No. 2018R1A2B5A02023190) for financial support.*

References

[1] T. S. Stashak, E. Farstvedt, A. Othic, *Clinical Techniques in Equine Practice* **3** (2004) 148–163. (https://doi.org/:10.1053/j.ctep.2004.08.006).

[2] E. Caló, V. V. Khutoryanskiy, *European Polymer Journal* **65** (2015) 252–267. (https://doi.org/-10.1016/j.eurpolymj.2014.11.024).

[3] J. Sun, H. Tan, *Materials* **6** (2013) 1285–1309. (https://doi.org/10.3390/ma6041285).

[4] A. Hebeish, M. Hashem, M. M. A. El-Hady, S. Sharaf, *Carbohydrate Polymers* **92** (2013) 407–413. (https://doi.org/10.1016/j.carbpol.2012.08.094).

[5] R. Jayakumar, M. Prabaharan, P. T. Sudheesh Kumar, S. V. Nair, H. Tamura, *Biotechnology Advances* **29** (2011) 322–337. (https://doi.org/10.1016/j.biotechadv.2011.01.005).

[6] S. Bhowmick, V. Koul, *Materials Science and Engineering: C* **59** (2016) 109–119. (https://doi.org/-10.1016/j.msec.2015.10.003).

[7] Ž. Jovanović, A. Krklješ, J. Stojkovska, S. Tomić, B. Obradović, V. Mišković-Stanković, Z. Kačarević-Popović, *Radiation Physics and* Chemistry **80** (2011) 1208–1215. (https://doi.org/10.1016/j.radphyschem.2011.06.005).
[8] T. T. T. Nguyen, B. Tae, J. S. Park, *Journal of Materials Science* **46** (2011) 6528–6537. (https://doi.org/10.1007/s10853-011-5599-0).
[9] A. Bal, F. E. Çepni, Ö. Çakir, I. Acar, G. Güçlü, *Brazilian Journal of Chemical Engineering* **32** (2015) 509–518.
[10] Y. Zhou, Q. Dong, H. Yang, X. Liu, X. Yin, Y. Tao, Z. Bai, W. Xu, *Carbohydrate Polymers* **168** (2017) 220–226. (https://doi.org/10.1016/j.carbpol.2017.03.044).
[11] D. Zhang, W. Zhou, B. Wei, X. Wang, R. Tang, J. Nie, J. Wang, *Carbohydrate Polymers* **125** (2015) 189–199. (https://doi.org/10.1016/j.carbpol.2015.02.034).
[12] J. Koehler, F. P. Brandl, A. M. Goepferich, *European Polymer Journal* **100** (2018) 1–11. (https://doi.org/10.1016/j.eurpolymj.2017.12.046).
[13] C. Ghobril, M. W. Grinstaff, *Chemical Society Reviews* **44** (2015) 1820–1835. (https://doi.org/10.1039/c4cs00332b).
[14] B. Obradovic, J. Stojkovska, Z. Jovanovic, V. Miskovic-Stankovic, *Journal of Materials Science: Materials in Medicine* **23** (2012) 99–107. (https://doi.org/10.1007/s10856-011-4522-1).
[15] K. Nešović, A. Janković, V. Kojić, M. Vukašinović-Sekulić, A. Perić-Grujić, K. Y. Rhee, V. Mišković-Stanković, *Composites Part B: Engineering* **154** (2018) 175–185. (https://doi.org/10.1016/j.compositesb.2018.08.005).
[16] M. D. Figueroa-Pizano, I. Vélaz, F. J. Peñas, P. Zavala-Rivera, A. J. Rosas-Durazo, A. D. Maldonado-Arce, M. E. Martínez-Barbosa, *Carbohydrate Polymers* **195** (2018) 476–485. (https://doi.org/-10.1016/j.carbpol.2018.05.004).
[17] J. M. A. Blair, M. A. Webber, A. J. Baylay, D. O. Ogbolu, L. J. V Piddock, *Nature Reviews Microbiology* **13** (2015) 42–51. (https://doi.org/10.1038/nrmicro3380).
[18] M. Berthet, Y. Gauthier, C. Lacroix, B. Verrier, C. Monge, *Trends in Biotechnology* **35** (2017) 770–784. (https://doi.org/10.1016/j.tibtech.2017.05.005).
[19] M. Rai, A. Yadav, A. Gade, *Biotechnology Advances* **27** (2009) 76–83. (https://doi.org/10.1016/j.biotechadv.2008.09.002).
[20] N. Duran, M. Duran, M. B. de Jesus, A. B. Seabra, W. J. Favaro, G. Nakazato, *Nanomedicine: Nanotechnology, Biology, and Medicine* **12** (2016) 789–799. (https://doi.org/10.1016/j.nano.2015.11.016).
[21] Q. L. Feng, J. Wu, G. Q. Chen, F. Z. Cui, T. N. Kim, J. O. Kim, *Journal of Biomedical Materials Research* **52** (2000) 662–668. (https://doi.org/10.1002/1097-4636(20001215)52:4<662::AID-JBM10>3.0.CO;2-3).
[22] Z. Jovanović, A. Radosavljević, Z. Kačarević-Popović, V. Mišković-Stanković, *Hemijska Industrija* **65** (2011) 687–696. (https://doi.org/10.2298/hemind110915064j).
[23] M. M. Abudabbus, I. Jevremović, A. Janković, A. Perić-Grujić, I. Matić, M. Vukašinović-Sekulić, D. Hui, K. Y. Rhee, V. Mišković-Stanković, *Composites Part B: Engineering* **104** (2016) 26–34. (https://doi.-org/10.1016/j.compositesb.2016.08.024).
[24] R. Surudžić, A. Janković, N. Bibić, M. Vukašinović-Sekulić, A. Perić-Grujić, V. Mišković-Stanković, S. J. Park, K. Y. Rhee, *Composites Part B: Engineering* **85** (2016) 102–112. (https://doi.org/10.1016/j.compositesb.2015.09.029).
[25] K. Nešović, A. Janković, T. Radetić, M. Vukašinović-Sekulić, V. Kojić, L. Živković, A. Perić-Grujić, K. Y. Rhee, V. Mišković-Stanković, *European Polymer Journal* (2019). (https://doi.org/10.1016/j.europolymj.2019.109257).
[26] K. Nešović, A. Janković, A. Perić-Grujić, M. Vukašinović-Sekulić, T. Radetić, L. Živković, S. J. Park, K. Yop Rhee, V. Mišković-Stanković, *Journal of Industrial and Engineering Chemistry* **77** (2019) 83–96. (https://doi.org/10.1016/j.jiec.2019.04.022).
[27] K. Nešović, V. Kojić, K. Y. Rhee, V. Mišković-Stanković, *Corrosion* **73** (2017) 1437–1447. (https://doi.-org/10.5006/2507).
[28] C. M. Hassan, N. A. Peppas, *Advances in Polymer Science* **153** (2000) 37–65. (https://doi.org/-10.1007/3-540-46414-X_2).
[29] S. R. Stauffer, N. A. Peppas, *Polymer* **33** (1992) 3932–3936. (https://doi.org/10.1016/0032-3861(92)90385-A).

[30] N. A. Peppas, S. R. Stauffer, *Journal of Controlled Release* **16** (1991) 305–310. (https://doi.org/10.1016/0168-3659(91)90007-Z).
[31] W. Stoks, H. Berghmans, P. Moldenaers., J. Mewis, *British Polymer Journal* **20** (1988) 361–369.
[32] K. Kawanishi, M. Komatsu, T. Inoue, *Polymer* **28** (1987) 980–984. (https://doi.org/10.1016/0032-3861(87)90173-X).
[33] M. M. Abudabbus, I. Jevremović, K. Nešović, A. Perić-Grujić, K. Y. Rhee, V. Mišković-Stanković, *Composites Part B: Engineering* **140** (2018) 99–107. (https://doi.org/10.1016/j.compositesb.2017.12.017).
[34] G. Merga, R. Wilson, G. Lynn, B. H. Milosavljevic, D. Meisel, *Journal of Physical Chemistry C* **111** (2007) 12220–12226. (https://doi.org/10.1021/jp074257w).
[35] A. Slistan-Grijalva, R. Herrera-Urbina, J. F. Rivas-Silva, M. Avalos-Borja, F. F. Castillon-Barraza, A. Posada-Amarillas, *Physica E: Low-Dimensional Systems and Nanostructures* **27** (2005) 104–112. (https://doi.org/10.1016/j.physe.2004.10.014).
[36] R. Desai, V. Mankad, S. K. Gupta, P. K. Jha, *Nanoscience and Nanotechnology Letters* **4** (2012) 30–34. (https://doi.org/10.1166/nnl.2012.1278).
[37] A. J. Haes, R. P. Van Duyne, *Journal of the American Chemical Society* **124** (2002) 10596–10604. (https://doi.org/10.1021/ja020393x).
[38] A. Slistan-Grijalva, R. Herrera-Urbina, J. F. Rivas-Silva, M. . Avalos-Borja, F. F. Castillon-Barraza, A. Posada-Amarillas, *Physica E* **25** (2005) 438–448. (https://doi.org/10.1016/j.physe.2004.07.010).
[39] J. Spasojević, A. Radosavljević, J. Krstić, D. Jovanović, V. Spasojević, M. Kalagasidis-Krušić, Z. Kačarević-Popović, *European Polymer Journal* **69** (2015) 168–185. (https://doi.org/10.1016/j.eurpolymj.2015.06.008).
[40] H. K. No, N. Y. Park, S. H. Lee, S. P. Meyers, *International Journal of Food Microbiology* **74** (2002) 65–72. (https://doi.org/10.1016/S0168-1605(01)00717-6).
[41] Y. Wu, Y. Yang, Z. Zhang, Z. Wang, Y. Zhao, L. Sun, *Advanced Powder Technology* **29** (2018) 407–415. (https://doi.org/10.1016/j.apt.2017.11.028).
[42] O. M. Bondarenko, M. Sihtmäe, J. Kuzmičiova, L. Ragelienė, A. Kahru, R. Daugelavičius, *International Journal of Nanomedicine* **13** (2018) 6779–6790. (https://doi.org/10.2147/IJN.S177163).
[43] M. Seong, D. G. Lee, *Current Microbiology* **74** (2017) 661–670. (https://doi.org/10.1007/s00284-017-1235-9).
[44] S. Rajeshkumar, L. V. Bharath, R. Geetha, *Broad spectrum antibacterial silver nanoparticle green synthesis: Characterization, and mechanism of action*, Elsevier Inc., 2019. (https://doi.org/10.1016/-b978-0-08-102579-6.00018-6).
[45] Y. Qing, L. Cheng, R. Li, G. Liu, Y. Zhang, X. Tang, J. Wang, H. Liu, Y. Qin, *International Journal of Nanomedicine* **13** (2018) 3311–3327. (https://doi.org/10.2147/IJN.S165125).
[46] H. J. Phillips, *Dye Exclusion Tests for Cell Viability*, Academic Press, Inc., 1973. (https://doi.org/10.1016/B978-0-12-427150-0.50101-7).
[47] G. Sjögren, G. Sletten, J. E. Dahl, *Journal of Prosthetic Dentistry* **84** (2000) 229–236. (https://doi.org/10.1067/mpr.2000.107227).